Electrical, magnetic and spectroscopic properties of tetrathiafulvalene charge transfer compounds with iron, ruthenium, rhodium and iridium halides

Young Inn Kim* and William E. Hatfield**
Department of Chemistry, The University of North Carolina at Chapel Hill, Chapel Hill, NC 27599-3290 (U.S.A.)

(Received March 11, 1991; revised May 16, 1991)

Abstract

The charge transfer compounds $(TTF)_2FeCl_3$, $(TTF)_3FeBr_3$, $(TTF)RuCl_3 \cdot 2H_2O$, $(TTF)RhCl_3 \cdot H_2O$ and $(TTF)IrCl_4 \cdot CH_3OH$ were prepared from reaction of solutions of TTF (tetrathiafulvalene) and the metal halide. Magnetic susceptibility and spectroscopic (electronic, vibrational, XPS and EPR) evidence indicate that there is incomplete charge transfer from the TTF donor to iron, and that there is essentially complete charge transfer to ruthenium, rhodium and iridium. The experimental evidence indicates that two electrons are transferred in the rhodium compound. The electrical conductivities of powdered samples of the iron compounds are five orders of magnitude greater than those of the ruthenium, rhodium and iridium compounds, being 6–10 S cm^{-1} at room temperature. All of the compounds exhibit semiconducting behavior which may be described by a mobility model having a temperature dependent preexponential term and relatively small activation energies.

Introduction

TTF (tetrathiafulvalene) is an excellent electron donor and forms charge transfer compounds which behave as organic metals [1]. The most famous of these compounds is TTF–TCNQ (TCNQ tetracyanoquinodimethane), a compound that exhibits high metallic conductivity which rises to almost 10^4 S cm^{-1} around 55 K [2, 3]. It has been concluded that compounds with high electrical conductivities should be formed from donor–acceptor molecules that are in partial oxidation (or mixed valence) states with uniform structures containing segregated stacks of the constituent molecules [1, 4]. Recently, charge transfer compounds of BEDT–TTF [bis(ethylenedithio)tetrathiafulvalene] and its analogs have received much attention [5]. Some of these BEDT–TTF salts exhibit superconductivity above 10 K [6–8].

Less attention has been paid to charge transfer salts with metal halide anions [9, 10]. In this study, TTF salts with iron, ruthenium, rhodium and iridium halides were prepared and characterized. TTF molecules in TTF–Fe halides were found to be partially oxidized, while the TTF–Ru, –Rh, and –Ir chloride compounds were found to be fully oxidized yielding simple salts. The compounds were characterized by electrical conductivity and magnetic susceptibility measurements, and by EPR, electronic, vibrational and X-ray photoelectron spectroscopy. The partially oxidized TTF salts exhibited electrical conductivities at room temperature that were five orders of magnitude greater than the simple salts.

Experimental

Synthesis

$(TTF)_2FeCl_3$ was prepared by the direct reaction of TTF and anhydrous $FeCl_3$. One mmol of anhydrous $FeCl_3$ was dissolved in a mixture of absolute methanol (20 ml) and trimethylorthoformate (4 ml). A solution of TTF (*c.* 3.5 mmol) in a mixture of methanol (20 ml) and trimethylorthoformate (4 ml) was added dropwise and the solution changed to a dark purple color immediately. The mixture was refluxed *c.* 1–2 h and then refrigerated overnight. Deep purple colored microcrystals precipitated. These were isolated by filtration and washed several times with absolute methanol. The microcrystalline precipitate was dried in vacuum at room temperature. $(TTF)_3FeBr_3$ was formed by an analogous method using anhydrous

---

*Current address: Department of Chemical Education, The Pusan National University, Pusan 609-735, Korea.

**Author to whom correspondence should be addressed.

0020-1693/91/$3.50

$FeBr_3$. (TTF)$RuCl_3 \cdot 2H_2O$ was also obtained by direct mixing a solution of hydrated $RuCl_3$ in methanol with an excess of TTF dissolved in methanol. The reaction mixture was refluxed *c.* 1–2 h. The precipitate that formed upon refrigeration was collected by filtration and dried in vacuum at room temperature. (TTF)$RhCl_3 \cdot H_2O$ and (TTF)$IrCl_4 \cdot CH_3OH$ were also formed by a similar method using hydrated $RhCl_3$ and $IrCl_4$, respectively. All of the compounds were dark purple in color. Elemental analysis was performed by Galbraith Laboratories, Inc., Knoxville, TN.

Anal. Calc. for $(TTF)_2FeCl_3$: C, 25.24; H, 1.40. Found: C, 25.29; H, 1.47%. Calc. for $(TTF)_3FeBr_3$: C, 23.79; H, 1.33. Found C: 24.55 H, 1.40%. Calc. for (TTF)$RuCl_3 \cdot 2H_2O$: C, 16.09; H, 1.80; Cl, 23.75. Found: C, 15.10; H, 1.69; Cl, 23.88%. Calc. for (TTF)$RhCl_3 \cdot H_2O$: C, 16.69; H, 1.40; Cl, 24.64. Found: C, 16.55; H, 1.45; Cl, 24.31%. Calc. for (TTF)$IrCl_4 \cdot CH_3OH$: C, 14.36; H, 1.14; Cl, 24.30. Found: C, 14.74; H, 1.41; Cl, 24.86%.

Physical measurements

Electrical resistivities were determined on compressed pellets (1.3 cm diameter, nominally 1 mm thick) by the Van der Pauw four-probe method [11] in the temperature range 20–300 K. The sample pellets were mounted on a ceramic insulating material and electrical connections to the sample pellet were made with four equally spaced (1.1 mm) spring-loaded electrodes. The sample pellet was spotted with conductive silver pasted to make a good contact. Low temperatures were obtained by using a CTI-Cryogenics model 21SC cryodine cryocooler. The temperature was measured with a DT-500k silicon diode connected to a Lake Shore Cryotronics, Inc. model DRC 80C temperature controller. Constant current was applied by using a Keithley model 227 current source and the voltage was measured with a Fluke 8502A multimeter.

EPR spectra of powdered samples were obtained with a Varian E-3 X-band spectrometer (≈ 9.5 GHz). The magnetic field of the E-3 was calibrated by using an NMR gaussmeter (Magnion model G-502) and a Hewlett-Packard precision frequency counter (model 5340A). The free radical DPPH ($g = 2.0036$) was used as a field marker in all cases. EPR data were collected at room temperature or at liquid nitrogen temperature (77 K).

Magnetic susceptibilities were measured from 4.2–77 K by using a Princeton Applied Research model 155 vibrating-sample magnetometer which was operated at 10 kOe. The magnetic susceptibility from 77 K to room temperature was collected with a Faraday Balance. The experimental methods have been described elsewhere [12]. The instruments were calibrated with $HgCo(SCN)_4$ [13]. The data were corrected for temperature independent paramagnetism and for the diamagnetism of the constituent atoms using Pascal's constants [14].

X-ray photoelectron spectra were taken on a Perkin-Elmer Physical Electronics model 5400 X-ray photoelectron spectrometer equipped with a magnesium anode X-ray source and a hemispherical analyzer, at a residual gas pressure of 5×10^{-9} torr. The samples were mounted on the fresh surface of indium foil to make good contact with the spectrometer. The binding energies (BE) were calibrated using the Au $4f_{7/2}$ peak at 84.9 eV and the Cu $2p_{3/2}$ peak at 932.4 eV. The adventitious C 1s line at 284.6 eV was used for charge referencing.

Electronic spectra were recorded on a Hewlett-Packard 8451 A spectrophotometer on solution or solid/Nujol mulls mounted between quartz plates. IR spectra (600–2000 cm^{-1}) were obtained using Nujol mulls on a sodium chloride plate or potassium bromide pellets with a Nicolet Model 20 DX FT-IR spectrophotometer.

Results and discussion

TTF–FeX_3 (X = Cl and Br) system

$(TTF)_2FeCl_3$ and $(TTF)_3FeBr_3$ were obtained by the reaction of excess TTF and anhydrous $FeCl_3$ and $FeBr_3$ in methanol, respectively. It will be shown that these compounds are charge transfer compounds with partially oxidized donors.

Electrical properties of TTF–FeX_3

Electrical resistivities (ρ) of TTF-FeX_3 were measured by the four-probe d.c. method where it was found that the resistivity increases as the temperature decreases. The temperature dependencies of the resistivities of the compounds are best described by the mobility model proposed by Epstein *et al.* [15]. The model incorporates a Boltzmann-like activation term and a temperature dependent preexponential term. The expression for the resistivity is

$$\rho(T) = AT^{+\alpha} \exp\left(\frac{E_a}{2kT}\right) \tag{1}$$

The Boltzmann factor describes the thermally activated generation of charge carriers in a narrow-bandgap semiconductor and the preexponential term ($T^{+\alpha}$) describes a temperature dependent mobility of charge carriers. The best-fit parameters calculated from eqn. (1) and the electrical conductivities at room temperature (σ_{RT}) are summarized in Table 1. Martinsen *et al.* have pointed out that the variation

TABLE 1. Electrical properties of TTF–metal halides

Compound	Conductivity[a] (S cm^{-1})	Best-fit parameters[b]		
		A	α	E_a (eV)
$(TTF)_2FeCl_3$	5.75×10^0	6.33×10^{-6}	6.03×10^{-1}	3.44×10^{-1}
$(TTF)_3FeBr_3$	9.65×10^0	2.59×10^0	5.65×19^{-1}	1.85×10^{-2}
$(TTF)RuCl_3\cdot2H_2O$	8.03×10^{-5}	1.19×10^{12}	3.20×10^0	1.77×10^{-2}
$(TTF)RhCl_3\cdot H_2O$	2.72×10^{-5}	5.99×10^5	5.10×10^{-1}	4.27×10^{-3}
$(TTF)IrCl_4\cdot CH_3OH$	1.06×10^{-4}	8.13×10^8	1.90×10	2.12×10^{-2}

[a] Conductivity was measured at room temperature. [b] The temperature dependence of resistivity may be described by the mobility model $\rho=AT^{+\alpha}\exp(E_a/2kT)$.

of A from crystal to crystal may be large, but that the α value and the activation energy for charge transport (E_a) are essentially constant in a related series [16]. The activation energies of the TTF–FeX_3 compounds are comparable to those of several organic conductors [17, 18].

The electrical conductivities (σ_{RT}) of TTF–FeX_3 at room temperature are in the order of 10^0 S cm^{-1}. These values are somewhat smaller than those of TTF [19] and BEDT–TTF [20] halide salts (10^1–10^2 S cm^{-1}) as single crystals, compounds which are known to have columnar structures of partially oxidized TTF and BEDT–TTF donor molecules. Schramm *et al.* [21] have reported that the conductivity of pelleted powder samples are smaller than single-crystal values along the molecular stacking direction by a factor of 10^2–10^3, as a result of interparticle contact resistance effects. In view of this expected effect, the conductivities of the TTF–FeX_3 salts are comparable to those of the TTF and BEDT–TTF halide salts. Such high conductivities in the TTF–FeX_3 salts demonstrate the partially oxidized nature of the TTF donor, and signal that low-dimensional phenomena are to be expected in TTF–FeX_3 compounds.

Magnetic properties of TTF–FeX_3

The ERP spectrum of a powdered sample of $(TTF)_3FeBr_3$ at room temperature exhibits a broad singlet at $g=2.117$ with a peak-to-peak linewidth (ΔH_{pp}) of 732 G. A narrow absorption signal at $g=2.002$ is superimposed on the broader band. The g value of this narrow absorption (<25 G) is nearly equal to the g value of the TTF free radical in solution ($g=2.0083$) [22]. This observation implies that the narrow band arises from the unpaired electron residing on TTF (or a TTF cluster) as a result of charge transfer to iron(III) bromide. The broad singlet did not acquire structure at 77 K although the g value shifted to 2.175 and the linewidth broadened somewhat yielding $\Delta H_{pp}=887$ G. The absorption is assigned to iron in $(TTF)_3FeBr_3$. The g values and the linewidth of TTF–FeX_3 compounds at 77 K are listed in Table 2, and for purposes of comparison EPR parameters of some conducting TTF compounds are listed in Table 3.

The observed linewidths of the TTF EPR signals in TTF–FeX_3 are less than 25 G. These values are somewhat less than the EPR linewidths in $TTF\cdot Br_{0.7}$ (≈40–52 G) and $TTF\cdot I_{0.7}$ (≈180–200 G). Sugano and Kuroda [23] have discussed the large linewidth in $TTF\cdot I_{0.7}$ and have concluded that the large linewidth is due to a strong spin–orbit coupling arising from the interaction of TTF and iodine. Meanwhile, the small linewidth in $TTF\cdot Cl_x$ (9 G) is caused by the considerable interaction along the one-dimensional TTF stacks rather than by the interaction between TTF and chlorine. Tomkiewicz and Taranko [19] have also explained the variation of the linewidth in TTF–halides in terms of the variation of the interstack coupling, where it was concluded that the smaller the linewidth, the larger the coupling among the TTF stacks. The observed linewidths in the TTF–FeX_3 compounds indicate that the interaction along the TTF stacks are significant and reflect the low-dimensional character of the materials. A similar result was also found in TTF–CuX_2 compounds [24].

The room temperature magnetic moments of $(TTF)_2FeCl_3$ and $(TTF)_3FeBr_3$ were found to be 4.75 and 5.05 BM, respectively. These values are very close to the spin-only value of 4.90 BM for four unpaired electrons, and the observation could be interpreted to imply that the oxidation state of iron in TTF–FeX_3 is +2 with a high-spin d^6 electronic configuration and that any contribution from paramagnetic TTF species is negligible as a result of band formation and Pauli temperature-independent paramagnetism only. However, the temperature dependence of the magnetic susceptibilities of the TTF–FeX_3 salts shown in Fig. 1 signal a much more complicated magnetic arrangement. The magnetic susceptibility of $(TTF)_3FeBr_3$ is almost temperature

TABLE 2. EPR parameters and magnetic properties of TTF–metal halides

Compound	EPR parameters		Magnetic moment[c] (BM)	Best-fit parameters[d]	
	g value[a]	EPR linewidth[b] (Gauss)		β	C_0
$(THF)_2FeCl_3$	$\langle g \rangle = 2.002$ (Fe) $\langle g \rangle = 1.988$ (TTF^+)	175 <25	4.75		
$(TTF)_3FeBr_3$	$\langle g \rangle = 2.175$ (Fe) $\langle g \rangle = 1.965$ (TTF^+)	887 <25	5.05		
$(TTF)RuCl_32H_2O$	$g_{zz} = 2.005$, $g_{xx} = 2.011$ $g_{yy} = 2.008$	10	1.03	4.92×10^{-2}	0.83
$(TTF)RhCl_3H_2O$	$\langle g \rangle = 2.009$	12	0.69	6.18×10^{-3}	0.61
$(TTF)IrCl_4CH_3OH$	$\langle g \rangle = 2.011$	10	0.66	6.94×10^{-3}	0.66

[a] The listed g values were measured at 77 K. [b] The values are peak-to-peak linewidth (ΔH_{pp}). [c] The magnetic moments were measured at room temperature. [d] The magnetic susceptibility was described by the power law, $\chi = C_0 T^{-\beta}$.

TABLE 3. EPR linewidth and g values of some TTF complexes

Compound	EPR linewidth	g_1	g_2	Reference
$TTF \cdot Cl_x$	9	2.0033	2.0097	19
$TTF \cdot Br_{0.7}$	40–52	2.0032	2.0108	23
$TTF \cdot I_{0.7}$	180–200	2.0050	2.0128	23
$(TTF)_{11}(SCN)_6$	11	2.0020	2.0088	25, 26
$(TTF)_{11}(SeCN)_6$	15	2.0022	2.0086	25, 27
$(TTF)_3CuCl_2$	17	1.9989	2.0049	24
$(TTF)_4CuBr_2$	12	2.0002	2.0074	24

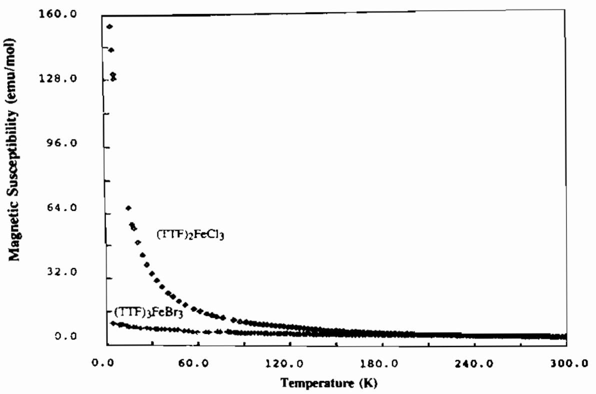

Fig. 1. Magnetic susceptibility data ($\times 10^4$) for $(TTF)_3FeBr_3$ (+) and $(TTF)_2FeCl_3$ (◇).

invariant while the magnetic susceptibility of $(TTF)_2FeCl_3$ increases as the temperature decreases.

A general model for the magnetic susceptibility of the $TTF–FeX_3$ salts must include a contribution from the unpaired electrons on the iron ion, a contribution from the electrons on TTF radicals, and the model must reflect exchange interactions between the various paramagnetic species. An appropriate expression that contains terms representing contributions from these magnetic sites is given below:

$$\chi_{(T)} = \chi_{Fe(T)} + \chi_{TTF} + \delta(T)$$
$$= C/(T - \theta) + \chi_{TTF} + \delta(T) \qquad (2)$$

This expression exhibits a Curie–Weiss term for the magnetic susceptibility from localized Fe spins, $\chi_{Fe(T)}$, a temperature independent term χ_{TTF}, associated with the unpaired electrons on the TTF radical [29], and an unprescribed temperature dependent term that accounts for exchange interactions.

Since localized paramagnetism on the iron ion may be expected to dominate and determine the observed magnetic susceptibility, a Curie–Weiss fit was attempted. The magnetic behavior of $(TTF)_2FeCl_3$ over the temperature range 4.2–290 K could not be described by the Curie–Weiss law with one set of parameters. In the high temperature region (90–290 K), a good fit to the curie–Weiss law is obtained with $C = 3.20$, $\theta = -42.6$ K and $g = 2.06$, and a magnetic moment of 5.05 BM is obtained from $\mu_{eff} = 2.828C^{1/2}$. A good fit to the data by the Curie–Weiss law in the temperature range 4.2–90 K is obtained with the parameters $C = 2.22$ and $\theta = -0.461$ K. A magnetic moment of 4.2 BM is obtained from $\mu_{eff} = 2.828C^{1/2}$. Attempts to fit the data with the more complicated model in eqn. (2) was not attempted because of the difficulty in choosing a δ(T) term that would reflect exchange interactions which are extremely important as reflected from the nearly temperature invariant magnetic susceptibility of $(TTF)_3FeBr_3$. The implications of the magnetic analysis for structural assignments are discussed in ‘Conclusions’.

Spectral properties of TTF–FeX$_3$

The oxidation state of the iron ion was investigated by X-ray photoelectron spectroscopy (XPS), since XPS is well known to be an excellent physical method for the determination of oxidation states in complex systems. The method involves the ionization of inner, core electrons by X-radiation. The binding energy (BE) of Fe $p_{3/2}$ core electrons for both (TTF)$_2$FeCl$_3$ and (TTF)$_3$FeBr$_3$ were measured to be 710.2 eV, a value that is significantly smaller, by 1.3 eV, than that of FeCl$_3$, and as shown in Table 4, comparable to the binding energy in FeCl$_2$ (and other iron(II) species [30]).

Electronic spectra of the TTF–FeX$_3$ complexes were recorded from 200–800 nm in both solution and the solid state. The results of the electronic spectra of the compounds are summarized in Table 5. Wudl *et al.* have reported the maximum absorbance (λ_{max}) of the TTF radical in H$_2$O at 340, 435 and 575 nm, with the TTF molecule exhibiting an absorption at 310 nm only [22]. The spectral data for the TTF–FeX$_3$ charge transfer salts are similar to those of the TTF radical, an observation that supports the conclusion that the TTF moiety in the TTF–FeX$_3$ salts are partially oxidized. The electronic spectrum of TTF$^+$Cl$^-$ in ethanol has also been reported and assigned as follows [31]: 340 ($b_{3g} \rightarrow b_{1u}$), 434 ($b_{2g} \rightarrow b_{1u}$) and 581 ($b_{2g} \rightarrow b_{1u}$) nm. These electronic transitions are comparable to the results found for the TTF–FeX$_3$ salts. Such low-energy absorption bands are typical of the intramolecular spectra of conjugated π-molecular radicals [31].

The absorption maxima of the electronic transitions in the TTF–FeX$_3$ salts in the solid state are shifted to higher energy with respect to the values in solution. For example, λ_{max} for (TTF)$_2$FeCl$_3$ at 578, 434 and 338 nm in solution are shifted to 552, 404 and 262 nm in the solid state. This energy shift reflects effects arising from increased interactions along the TTF$^+$ stacks in the solid state. A comparable effect is also observed for TFF$^+$ dimers in solid state samples of TTF–Cl [31].

IR spectra of the TTF–FeX$_3$ salts were obtained by using Nujol mulls on sodium chloride plates. The spectra exhibited a very broad intense band extending from 1000–4000 cm^{-1}. These intense absorptions arise from the band structure of these semiconductors [32] and masks many of the vibrational modes of the compounds. Such effects are commonly observed in highly conductive charge transfer salts [33]. A limited number of vibrational bands of TTF in the TTF–FeX$_3$ salts were found in the absorption tail in the range of 600–1400 cm^{-1}. The vibrational modes from which these bands arise were tentatively assigned by comparing their positions and intensities with reported spectra of one-dimensional TTF compounds [34]. The spectral bands and their assignments are listed in Table 5.

In (TTF)$_2$FeCl$_3$, the absorption bands at 1075 and 825 cm^{-1} were assigned to the ν_{15} (CCH bend in

TABLE 4. Binding energy (eV) of TTF–metal halides

Compound	Metal					Cl (2p)	S (2p)	O (1s)
	$p_{3/2}$	$d_{3/2}$	$d_{5/2}$	$f_{5/2}$	$f_{7/2}$			
FeCl$_3$	711.5							
FeCl$_2$	710.8							
(TTF)$_2$FeCl$_3$	710.2					197.9	163.8 (2.5)[a]	
(TTF)$_3$FeBr$_3$	710.2						163.9 (2.7)	
RhCl$_3$xH$_2$O	499.4 (3.15)	314.6 (2.01)	309.8 (1.70)			198.8		533.3
(TTF)RhCl$_3$·H$_2$O	497.8 (2.86)	313.4 (1.59)	308.7 (1.39)			197.3	163.8	532.2
IrCl$_4$·xH$_2$O			297.5 (4.54)	64.9 (1.50)	62.0 (1.47)	198.7		532.6
(TTF)IrCl$_4$·CH$_3$OH			297.0 (4.09)	64.4 (1.31)	61.4 (1.38)	197.3	163.9 (2.7)	532.1
RuCl$_3$·xH$_2$O		286.4 (1.89)	282.0 (1.70)			198.6		532.2
(TTF)RuCl$_3$·2H$_2$O		285.6 (1.80)	281.3 (1.65)			198.2	164.3 (2.7)	

[a]FWHM (full width at half maximum) of the peak is given in parentheses.

TABLE 5. Electronic and IR spectra of TTF–metal halides

Compound	Electronic spectra[a]			IR spectra[b] (cm^{-1})
	λ_{max} (nm)		Solvent	
$(TTF)_2FeCl_3$	198(3.3×10^4)	338(1.0×10^4)	H_2O	815(ν_{23}) 825(ν_{16}) 1075(ν_{15})
	434(2.3×10^4)	578(6.2×10^3)		1237(ν_{23})
	210, 262, 404, 552		solid/nujol	
$(TTF)_3FeBr_3$	198(4.9×10^4)	338(8.7×10^3)	H_2O	815(ν_{25}) 827(ν_{16}) 1233(ν_{23})
	432(1.7×10^4)	578(4.4×10^3)		
	210, 264, 378, 560		solid/nujol	
$(TTF)RuCl_3$	306(5.3×10^3)	366(sh, 3.0×10^3)	DMSO	696(m, ν_{34}) 746(m, ν_{17})
	422, 542		solid/nujol	798(w, ν_{25}) 829(m, ν_{16})
				940(w) 1089(w, ν_{15}) 1256(w, ν_{23})
				1346(s) 1471(m, ν_{14}) 1505(ν_2)
				1608(m, br)
$(TTF)RhCl_3\cdot H_2O$	298(8.0×10^3)	375(sh, 3.2×10^3)	DMSO	690(m, ν_{34}) 748(w, ν_{17}) 770(w)
	488(sh, 8.8×102)			798(w, ν_{25}) 824(m, ν_{16}) 862(w)
	248, 407		solid/nujol	938 1020(w) 1054(w)
				1089(m, ν_{15}) 1255(m, ν_{23}) 1350(s)
				1450(s, ν_{14}) 1614(s) 1716(m)
$(TTF)IrCl_4\cdot CH_3OH$	322(6.8×10^3)	374(sh, 3.2×10^3)	DMSO	709(w) 732(w) 805(w, ν_{25})
	433(sh, 1.0×10^2)		solid/nujol	823(w, ν_{16}) 1262(w, ν_{23}) 1350(s)
	430, 544			1465(m, ν_{14}) 1623(m)

[a]Extinction coefficient (ϵ) are listed in parentheses. [b]s, strong; m, medium; w, weak; br, broad.

TTF ring) and ν_{16} (CS stretch), respectively. The observed values are between those reported for the TTF molecule (ν_{15}: 1090, ν_{16}: 781 cm^{-1}) and the TTF free radical (ν_{15}: 1072, ν_{16}: 836 cm^{-1}) [34], thus providing further evidence of the partial oxidation of the TTF molecule in $(TTF)_2FeCl_3$. Similar results were observed for the $(TTF)_3FeBr_3$ salt.

TTF–Ru, –Rh, –Ir chlorides

TTF–Ru, –Rh and –Ir chlorides were prepared by the direct reaction of TTF and hydrated $RuCl_3$, $RhCl_3$ and $IrCl_4$, respectively. One-electron transfer was observed from TTF to Ru(III) and Ir(IV) chlorides to produce $(TTF)Ru(II)Cl_3\cdot 2H_2O$ and $(TTF)Ir(III)Cl_4\cdot CH_3OH$, respectively, with the metal ion in a stable d^6 electronic configuration. Two-electron transfer was observed in $(TTF)RhCl_3\cdot H_2O$. It is known that Rh(III) is typically reduced to Rh(I) rather than to Rh(II) due to the large ligand field stabilization energy [35]. Furthermore, the standard reduction potential of Rh (Rh(III) → Rh(I), $E_{1/2}=0.975$ V versus SCE) is comparable with that of Ru (Ru(III) → Ru(II), $E_{1/2}=0.86$ V) and Ir (Ir(IV) → Ir(III), $E_{1/2}=0.867$ V) in acid solution [36]. As a result of electron transfer from TTF to the metal in the reaction, TTF is complete ionized to either TTF$^+$ or TTF^{2+}. TTF^{2+} salts as well as TTF$^+$ salts are well known [37].

Electrical properties

The temperature-dependences of the electrical resistivities of pelleted powder samples of TTF–Ru, –Rh and –Ir chlorides were measured from 10 K to room temperature. The electrical resistivity of TTF–Ru chloride increases as the temperature decreases in the range of 300–63 K. The resistivity reaches a maximum value ($\rho_{max}=2.8\times10^5$ Ω cm) at 63 K and then decreases until it becomes nearly constant ($\rho=2.0\times10^5$ Ω cm) at 38 K and below. TTF–Ir chloride exhibits similar behavior qualitatively, reaching a maximum resistivity ($\rho_{max}=4.6\times10^4$ Ω cm) at 58 K.

The temperature responses of the resistivity of TTF–Rh chloride is somewhat different. As the temperature is lowered from 300 K, the resistivity of TTF–Rh chloride decreases with a decrease in temperature with a minimum in resistivity ($\rho_{min}=3.4\times10^4$ Ω cm) occurring at 230 K. Below 230 K, the resistivity increases with a decrease in temperature reaching a maximum ($\rho_{max}=4.9\times10^4$ Ω cm) at 53 K. The resistivity then decreases with decreasing temperature and at 38 K reaches a constant value ($\rho=4.1\times10^4$ Ω cm).

The electrical conductivities at room temperature of TTF–Ru, –Rh and –Ir chlorides are in the order of 10^{-4} to 10^{-5} S cm^{-1}, values that are much smaller than those of TTF–FeX_3 compounds. The difference in electrical properties arises from the fact that TTF in TTF–Ru, –Rh and –Ir chlorides are fully ionized, where TTF in TTF–FeX$_3$ are only partially ionized to give complex charge transfer salts [4, 38]. For example, the room temperature conductivities of the simple and complex salts of *N*-methylquinolinium and *N*-methylacridinium TCNQ differ by more than four orders of magnitude [39, 40]. The temperature dependent resistivities were described well by the mobility model, eqn. (1), in the temperature range in which the compounds exhibited semiconducting behavior, that is, in the region in which the resistivity increased with a decrease in temperature. The best-fit parameters of the parameters in eqn. (1) are listed in Table 1. These parameters are comparable to those exhibited by other conducting systems with stacked organic radicals [41, 42], and the room temperature conductivities are comparable to those of TTF–Pt and –Cu oxalate compounds [43] which are known to have columnar structures of TTF radical cations. Additional evidence for stacks of TTF radicals is provided by the magnetic and spectroscopic investigations described in the following sections.

Magnetic properties

The TTF–Ru, –Rh and –Ir chlorides were also examined by EPR spectroscopy. The EPR spectra of powdered samples of TTF–Rh and –Ir chlorides exhibited symmetric singlets at about $\langle g \rangle = 2$ both at room temperature and at 77 K. TTF–Ru chloride gave an unsymmetrical shaped spectrum with $g_{\parallel} = 2.011$ and $g_{\perp} = 2.005$ at room temperature, but upon lowering the temperature to 77 K, three g values were observed at $g_{xx} = 2.011$, $g_{yy} = 2.008$ and $g_{zz} = 2.005$. These three g values average to 2.008, a value that is nearly equal to the value of TTF radical in solution ($g = 2.00838$) [22] and to the values observed for a selection of salts containing the TTF donor, those being $g = 2.0073$–2.0081 [27]. EPR signals attributable to the metal ion in TTF–Ru, –Rh and –Ir chlorides were not detected. The absence of a metal ion signal implies that any unpaired electrons are distributed on TTF and that the metal atoms in each compound are diamagnetic: low-spin octahedral Ru(II) d^6, square planar Rh(I) d^8 and octahedral low-spin Ir(III) d^6.

EPR spectral results for several TTF charge transfer salts are listed, for comparison, in Table 3. The observed linewidths of TTF–Ru, –Rh and –Ir chlorides are 10–12 G, values which are comparable to those of (TTF)$_{11}$(SCN)$_6$ and (TTF)$_{11}$(SeCN)$_6$ [26]. These similarities of EPR spectral properties [44] indicate that there are significant interactions between TTF radicals along the stacks in TTF–Ru and –Ir chlorides. The presence of an EPR signal in TTF–Rh chloride indicates that there are paramagnetic sites in the TTF stacks presumably from defects, or from incomplete charge transfer, although the latter contribution is not great.

The temperature dependences of the magnetic susceptibilities of TTF–Ru, –Rh and –Ir chlorides are shown in Fig. 2. The magnetic susceptibility increases slowly as the temperature decreases. The data can not be described by the Curie–Weiss law but do follow the power law $\chi = C_0 T^{-\beta}$, where β is less than 1. The magnetic susceptibility data for quinolinium–(TCNQ)$_2$ [45] and (tetramethyl-*p*-phenylenediamine)–TCNQF$_4$ [46] also behave according to this power law, with β ranging from 0.72–0.85.

Spectroscopic properties

XPS spectra of the metal ion in TTF–Ru, –Rh and –Ir chlorides were collected and the data are summarized in Table 4. Although the binding energy is known to be affected by the different chemical circumstances such as stereochemistry, ligand electronegativity and delocalization of the charge on the ligand, among other effects, the oxidation state plays an important role on the magnitude of the shift of the binding energy. In general it may be concluded that the larger the binding energy, the higher the oxidation state as a result of lower electron density on the atom or ion [47]. As shown in Table 4, the binding energies of the metal core electrons in TTF–Rh, –Ir and –Ru chlorides are about one eV less than those of the hydrated Rh(III), –Ir(IV) and –Ru(III) chlorides, respectively. These observations suggest lower oxidation states of the metal ion in the TTF–Rh, –Ir and –Ru chloride charge transfer compounds. In the charge transfer reactions, the metal was reduced by the TTF donor to the lower oxidation state.

The binding energies of the chlorine 2p electrons also reflect the oxidation state of the metal ion. For

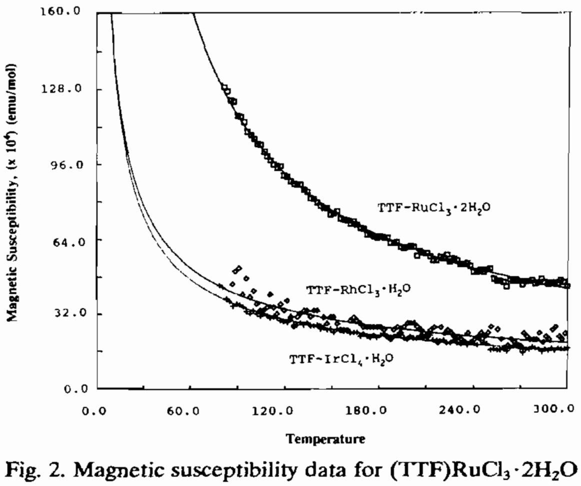

Fig. 2. Magnetic susceptibility data for (TTF)RuCl$_3$·2H$_2$O (□), (TTF)RhCl$_3$·H$_2$O (◇) and (TTF)IrCl$_4$·CH$_3$OH (+).

example, the binding energy of Cl 2p in (TTF)–Rh chloride is 197.3 eV, a value that is less than the value of 198.8 eV in $RhCl_3\cdot xH_2O$. This observation indicates that there is more electron density on chloride in TTF–Rh chloride than in $RhCl_3\cdot 2H_2O$ as a result of the lower oxidation state of the metal ion.

A binding energy for Rh $d_{5/2}$ in triphenylphosphine–Rh(I) chloride of 307.2–308.2 eV has been reported, whereas the similar Rh(III) compound exhibits a binding energy over 309 eV [48]. Rhodium(III)–glycine complexes also exhibit binding energies in the range of 310.5–310.8 eV [49]. The binding energy of Rh $d_{5/2}$ in TTF–Rh chloride was found to be 308.7 eV. This observation provides evidence of oxidation state rhodium(I) in the TTF charge transfer salt, since the binding energy is in the range exhibited by Rh(I) compounds (307.6–309.6 eV) [50]. The binding energy of Ru $d_{5/2}$ in TTF–Ru chloride (281.3 eV) is close to that of $[Ru^{II}(bipyridine)_3]Cl_2\cdot xH_2O$ (281.6 eV) [51], but the value is larger than those exhibited by many ruthenocenes (279.6–280.8 eV) [52].

Efforts to distinguish the oxidation state of TTF by XPS were inconclusive. There was essentially little change in the sulfur 2p binding energies in the compounds examined. This observation was not unexpected in view of electron density calculations on TTF and related compounds [53], and examinations of spectral features of the compounds [54].

The oxygen 1s peak from the water molecules in each compound was observed in the range of 532.1–532.3 eV. The binding energy of oxygen 1s in coordinated water is known to be -534 eV, a value that is much higher than that of lattice water of hydration [55]. A strict interpretation of the binding energy of the oxygen 1s electrons in TTF–Rh, –Ir and –Ru chlorides would suggest that the water molecules are not coordinated. This observation has important implications concerning structural assignments. If the water molecules are not coordinated, then in order to fulfil the coordination requirements of the metal ions, sulfur donor atoms from the TTF stacks must be involved. This conclusion is important with regard to the assignment of structures to the $TTF–FeX_3$ charge transfer compounds.

TABLE 6. ν_{14} and ν_{16} vibrational modes of selected TTF complexes

Compound	ν_{14} (cm^{-1})	ν_{16} (cm^{-1})	Reference
$(TTF)_2FeCl_3$		825	this work
$(TTF)_3FeBr_3$		827	this work
$(TTF)RuCl_3\cdot 2H_2O$	1465	829	this work
$(TTF)RhCl_3\cdot H_2O$	1450	824	this work
$(TTF)IrCl_4\cdot CH_3OH$	1471	823	this work
TTF	1530	781	34
$(TTF)^+Br^-$	1478	836	34
$(TTF)^+HgCl_3{}^-$	1490		10
$(TTF)^{2+}(BF_4{}^-)_2$	1440		37
$(TTF)^{2+}[CuCl_4]^{2-}$	1425		37
$(TTF)_2{}^+[CuCl_4]^{2-}$	1495		37

Electronic spectral data for TTF–Ru, –Rh and Ir chlorides are listed in Table 5. The electronic spectrum of TTF–Rh chloride in the solid state differs from that of TTF–Ru and –Ir chlorides in that the low energy band above 500 nm is not present in TTF–Rh chloride. It has been shown [37] that the TTF^+ cation in TTF–copper and gold chloride complexes exhibits λ_{max} at 435 nm and 500–600 nm, whereas the TTF^{2+} ion has a characteristic absorption only at 445–460 nm in the solid state. The absence of the low energy band in TTF–Rh chloride is consistent with the formulation of the material as containing dicationic TTF^{2+}. Additional evidence for the presence of TTF^{2+} is provided by the IR spectra described below.

The IR spectra in KBr pellets of TTF–Ru, –Rh and –Ir chlorides are summarized in Table 6. The assignments of the vibrational modes were made by comparing the data for the present compounds with the data reported by Bozio *et al.* [34]. Of the C–C stretching bands in the five membered TTF ring, the ν_{14} mode has been observed to undergo large shifts of approximately 50 cm^{-1} per unit charge on oxidation of TTF [34]. A similar shift to a higher frequency of the C–C stretching bands as the negative charge increases has also been found in 1,2-dithiolato complexes [56]. The ν_{14} bands in $(TTF)_1RuCl_3\cdot 2H_2O$ and $(TTF)_1IrCl_4\cdot CH_3OH$ are shifted *c.* 60 cm^{-1} with respect to the TTF molecule (1530 cm^{-1}), a shift that is comparable to that seen in TTF^+Br^- (1478 cm^{-1}). The value of ν_{14} in $(TTF)_1RhCl_3\cdot H_2O$ is close to that in $TTF^{2+}(BF_4)_2$ (1440 cm^{-1}). This observation as well as electronic spectra demonstrate that TTF exists as a dication in TTF–Rh chloride and as a monocation in TTF–Ru and –Ir chlorides.

Conclusions

The relatively high electrical conductivities, and the similarities of the spectral properties to those of other compounds containing TTF stacks, lead to the conclusion that the charge transfer salts and compounds produced in this work also have stacked TTF chains. The ruthenium and iridium chloride compounds have stacks of TTF^+ monocations, while the rhodium compound has stacks of TTF^{2+} dications. The magnetic properties reveal charge transfer to the metal ions resulting in diamagnetic electronic configurations, and the magnetic properties also reflect significant interactions between the TTF$^+$ radical cations in the stacks. The temperature dependence of the magnetic susceptibilities and spectroscopic properties indicate that paramagnetic states are thermally accessible above the conduction band. Anomalies in the electrical properties for the Rh, Ir and Ru compounds near 38 K for the Ru and Rh compounds and near 58 K for the Ir compound suggest phase transitions which are common in TTF compounds [1].

The metal ions are diamagnetic in the series of TTF–Ru, –Rh and –Ir chlorides where the metal ions have d^6 electronic configurations in the ruthenium(II) and iridium(III) compounds and d^8 in the rhodium(I) compound. In order to fulfil coordination number requirements, the metal ions are coordinated to the sulfur donor atoms in the TTF stacks. This latter conclusion has significance with regard to the structures and magnetic properties of the iron(II) compounds.

The spectral properties of the TTF–FeX$_3$ compounds are consistent with stacked TTF$^{\delta+}$ radicals with the –FeX$_3$$^{\delta-}$ entities bonded to the sulfur donor atoms of the TTF$^{\delta+}$ stacks in order to fulfil the coordination number requirement of the iron(II) ions. The magnetic properties of the TTF–FeX$_3$ compounds relect magnetic interactions, and these interactions must arise from exchange between the TTF$^{\delta+}$ radicals in the stacks as well as between the high-spin iron(II) ions and the TTF radical electrons, with the interaction being much greater in TTF–FeBr$_3$ than in TTF–FeCl$_3$. This interaction is reflected in the electrical conductivity properties with the resistivity of TTF–FeBr$_3$ being significantly greater than that of TTF–FeCl$_3$. This observation may be useful in the design of molecular-based materials with prescribed electrical and magnetic properties.

Acknowledgement

This research was supported in part by the Office of Naval Research.

References

1 W. E. Hatfield, *Molecular Metals,* NATO Conference Series, Plenum, New York, 1979.

2 L. G. Coleman, M. J. Cohen, D. J. Sandman, F. G. Yamagishi, A. F. Garito and A. J. Heeger, *Solid State Commun.,* (1973) 1125.

3 J. Ferraris, O. O. Cowan, V. Valatka, Jr. and J. H. Perlstein, *J. Am. Chem. Soc., 95* (1973) 948.

4 J. B. Torrance, *Acc. Chem. Res., 12* (1979) 79.

5 J. M. Williams, H. H. Wang, T. J. Emge, U. Geiser, M. A. Beno, P. C. W. Leung, K. D. Carlson, R. J. Thorn, A. J. Schultz and M. H. Wangbo, *Prog. Inorg. Chem., 35* (1987) 51, and refs. therein.

6 R. P. Shibaeva, V. F. Kaminskii and E. B. Yagubskii, *Mol. Cryst. Liq. Cryst., 118* (1985) 361.

7 J. M. Williams, T. J. Emge, H. H. Wang, M. A. Beno, P. T. Copps, L. N. Hall, K. D. Carlson and G. W. Crabtree, *Inorg. Chem., 23* (1984) 2558.

8 K. D. Carlson, G. W. Crabtree, M. Choi, L. N. Hall, P. T. Copps, H. H. Wang, T. J. Emge, M. A. Beno and J. M. Williams, *Mol. Cryst. Liq. Cryst., 125* (1985) 145.

9 K. Kondo, G. Matsubayashi, T. Tanaka, H. Yoshioka and K. Nakatsu, *J. Chem. Soc., Dalton Trans.,* (1984) 379, and refs. therein.

10 T. J. Kistenmacher, M. Rossi, C. C. Chiang, R. P. Van Duyne and A. R. Siedle, *Inorg. Chem., 19* (1980) 3604.

11 J. L. Van der Pauw, *Philips Res. Rep., 13* (1958) 1.

12 D. B. Brown, J. A. Zubieta, P. A. Vella, J. T. Wrobleski, T. Watt, W. E. Hatfield and P. Day, *Inorg. Chem., 19* (1980) 1945.

13 D. B. Brown, V. H. Crawford, J. W. Hall and W. E. Hatfield, *J. Phys. Chem., 81* (1977) 1303.

14 E. Konig, *Magnetic Properties of Coordination and Organometallic Transition Metal Complexes,* Springer, Berlin, 1966.

15 A. J. Epstein, E. M. Conwell, D. J. Sandman and J. S. Miller, *Solid State Commun., 23* (1977) 355.

16 J. Martinsen, L. J. Pace, T. E. Phillips, B. M. Hoffman and J. A. Ibers, *J. Am. Chem. Soc., 104* (1982) 83.

17 P. A. Berger, D. J. Dahm, G. R. Johnson, M. G. Miles and J. D. Wilson, *Phys. Rev. B, 12* (1975) 4085.

18 J. S. Miller and A. J. Epstein, *Ann. N.Y. Acad. Sci.,* (1978) 313.

19 Y. Tomkiewicz and A. R. Taranko, *Phys. Rev. B, 18* (1978) 733.

20 S. S. P. Parkin, E. M. Engler, V. Y. Lee and R. R. Schumaker, *Mol. Cryst. Liq. Cryst., 119* (1985) 375.

21 C. J. Schramm, R. P. Scaringe, D. R. Stojakovic, B. M. Hoffman, J. A. Ibers and T. J. Marks, *J. Am. Chem. Soc., 102* (1980) 6702.

22 F. Wudl, G. M. Smith and E. J. Hufnagel, *J. Chem. Soc., Chem. Commun.* (1970) 1453.

23 T. Sugano and H. Kuroda, *Chem. Phys. Lett., 47* (1977) 92.

24 Y. I. Kim and W. E. Hatfield, unpublished results.

25 F. Wudl, D. E. Schafer, W. M. Walsh, Jr., L. W. Rupp, F. J. DiSalvo, J. V. Vaszczuk, M. C. Kaplan and G. A. Thomas, *J. Chem. Phys., 66* (1977) 377.

26 Y. Tomkiewicz and E. M. Engler, *Bull. Am. Phys. Soc., 20* (1975) 479.

27 L. Carara, F. Gerson, D. O. Cowan and K. Lerstrup, *Helv. Chim. Acta, 97* (1985) 201.

28 Y. Tomkiewicz, B. A. Scott, L. J. Tao and R. S. Title, *Phys. Rev. Lett., 21* (1974) 1363.

29 B. M. Hoffman and J. A. Ibers, *Acc. Chem. Res., 16* (1983) 15.

30 C. D. Wagner, W. M. Riggs, L. E. Davis, J. F. Moulder and G. E. Muilenberg, *Handbook of X-ray Photoelectron Spectroscopy,* Perkin-Elmer, Eden Prairie, MN, 1979.

31 J. B. Torrance, B. A. Scott, B. Welber, F. B. Kaufman and P. E. Seiden, *Phys. Rev. B, 19* (1979) 730.

32 M. J. Rice, L. Peitronero and P. Briiesch, *Solid State Commun.*, *21* (1977) 757.

33 R. C. Wheland and J. L. Gillson, *J. Am. Chem. Soc.*, *98* (1976) 3916.

34 R. Bozio, I. Zanon, A. Girlando and C. Pecile, *J. Chem. Phys.*, *71* (1979) 2282.

35 F. A. Cotton and G. Wilkinson, *Advanced Inorganic Chemistry*, Wiley, New York, 5th edn., 1988.

36 A. J. Bard, R. Parsons and J. Jordon, *Standard Potentials in Aqueous Solution*, IUPAC, Marcel Dekker, New York, 1985.

37 A. R. Seidle, T. F. Candela, T. F. Finnegan, R. P. Van Duyne, T. Cape, G. F. Kokoszka, P. M. Woyciejes and J. A. Hashmall, *Inorg. Chem.*, *20* (1981) 2635.

38 A. F. Garito and A. J. Heeger, *Acc. Chem. Res.*, *7* (1974) 232.

39 W. J. Siemons, P. E. Bierstedt and R. G. Kepler, *J. Chem. Phys.*, *39* (1963) 3523.

40 L. R. Melby, *Can. J. Chem.*, *43* (1965) 1448.

41 T. E. Phillips, R. P. Scaringe, B. M. Hoffman and J. A. Ibers, *J. Am. Chem. Soc.*, *102* (1980) 3435.

42 J. Martinsen, L. J. Pace, T. E. Phillips, B. M. Hoffman and J. A. Ibers, *J. Am. Chem. Soc.*, *104* (1984) 83.

43 K. Ueyama, A. Tanaka, G. Matsubayashi and T. Tanaka, *Inorg. Chim. Acta*, *97* (1985) 201.

44 R. B. Somoano, A. Gupta and V. Hadek, *J. Chem. Phys.*, *63* (1975) 4970.

45 L. C. Tippi and W. G. Clark, *Phys. Rev. B*, *23* (1981) 5846.

46 Z. G. Soos, H. J. Keller, K. Ludolf, J. Queckborner, D. Wehe and S. Flandrois, *J. Chem. Phys.*, *74* (1981) 5287.

47 S. Srivastava, *Appl. Spectrosc. Rev.*, *22* (1986) 401.

48 P. G. Gassman, D. W. Macomber and S. M. Willging, *J. Am. Chem. Soc.*, *107* (1985) 2380.

49 V. I. Nefedov, I. V. Promofeva, A. E. Bukonova, L. N. Schubochkin, Y. C. Salyn and C. L. Pershin, *Russ. J. Inorg. Chem.*, *19* (1974) 859.

50 S. L. T. Anderson, K. L. Watters and R. F. Howe, *J. Catal.*, *69* (1981) 212.

51 W. H. Quayle and J. H. Lunsford, *Inorg. Chem.*, *21* (1982) 97.

52 P. G. Gassman and C. H. Winter. *J. Am. Chem. Soc.*, *110* (1988) 6130.

53 R. Zahradnito, P. Carsky, S. Hunig, G. Kiesslich and D. Schentzow, *Int. J. Sulfur Chem., Part C*, *6* (1971) 109.

54 I. Irkemoto, M. Yamada, T. Sugano and H. Kuroda, *Bull. Chem. Soc. Jpn.*, *53* (1980) 1871.

55 K. Yokoyama, G. Matsubayashi and T. Tanaka, *Polyhedron*, *7* (1988) 1063.

56 C. W. Schlapfer and K. Nakanoto, *Inorg. Chem.*, *14* (1975) 1338.